Journal of Applied Geophysics 225 (2024) 105377

Contents lists available at ScienceDirect

Journal of Applied Geophysics

journal homepage: www.elsevier.com/locate/jappgeo

Near real-time nautical depth mapping via horizontal optical fibers and distributed acoustic sensing

Menno Buisman [a,b,*], Deyan Draganov [a], Alex Kirichek [c]

[a] Section of Applied Geophysics and Petrophysics, Department of Geoscience & Engineering, Faculty of Civil Engineering & Geosciences, Delft University of Technology, Engineering, Stevinweg 1, 2628 CN Delft, the Netherlands
[b] Port of Rotterdam, Wilhelminakade 909, 3072 AP Rotterdam, the Netherlands
[c] Section of Rivers, Ports, Waterways and Dredging Engineering, Department of Hydraulic Engineering, Faculty of Civil Engineering & Geosciences, Delft University of Technology, Stevinweg 1, 2628 CN Delft, the Netherlands

ARTICLE INFO

Keywords:
Distributed acoustic sensing
Nautical depth
Monitoring
Passive sources

ABSTRACT

Safe navigation in ports and waterways subjected to siltation requires nautical depth monitoring. For this purpose, surveying vessels equipped with a zero-offset echo sounder and intrusive point measurements are frequently used. Because these measurements depend on the availability of a surveying vessel and require access to quay walls, such as at the container terminals in seaports, the temporal resolution is limited. Especially at these locations, a high temporal resolution monitoring system could allow for a higher occupancy rate. We propose to use Distributed Acoustic Sensing to monitor the nautical depth using fiber-optical cables. We install five horizontal fibers at different heights between two points and continuously record along the complete installation. Analysing the continuous recordings, we show that horizontal fibers can be used to monitor the water-mud interface depth with a vertical resolution around six mm. Multiple passive sources, like vessel movements and water currents, are used to estimate the water-mud interface.

1. Introduction

Ports and waterways with high siltation rates require frequent surveying to ensure the nautical depth. In seaports with a low energetic environment, sedimentation frequently comes as large quantities of fine sediments, creating thin layers of a highly aqueous suspension known as fluid mud. The density of fluid mud is frequently used by port authorities worldwide for the nautical criterion (McAnally et al., 2007a; Kirichek et al., 2018). At the same time, fluid mud makes the depth measurements ambiguous since its density gradually increases from water, being 1 kg/l, to consolidated mud, with 1.3 kg/l. Furthermore, the relation between shear stresses and density in mud is non-linear (McAnally et al., 2007a), which is why different port authorities in various places defined their nautical bottom criterion based on local sediment characteristics and hydrodynamics (Kirichek et al., 2018). Currently, surveying techniques mainly rely on acoustic methods (McAnally et al., 2007b) in the form of dual- or multi-frequency echo sounders. Echo sounders operate as both a source and receiver, measuring the two-way travel time from the source to the bottom and back to the receiver. An accurate velocity model is then used to convert the two-way travel time to depth (McAnally et al., 2007b). However, at specific locations with a mixture of sea and river water, such as estuaries, obtaining an accurate velocity profile is most challenging because of different P-wave velocities in the water column, leading to time-consuming calibration work and a higher inaccuracy.

Additionally, the results of these echos-sounders are frequently inaccurate due to the dim reflection(s) related to the small acoustic-impedance contrast between water and fluid mud since fluid mud can have a gradual increase in density, while settling and consolidating, and a longitudinal-wave velocity approximately 3% - 9% higher than that of water (Ma et al., 2022). These surveying techniques have low repeatability and are restricted by the availability of a surveying vessel and quay wall access. Especially at the financially crucial quay walls, availability for surveying is severely constrained due to the high costs of halting activities for a surveying vessel. Finally, substantial changes in the nautical depth can often occur after storms, implying that extensive, time-consuming surveys are required again to ensure the safe navigability of vessels. These surveys are time-consuming due to the large

* Corresponding author at: Section of Applied Geophysics and Petrophysics, Department of Geoscience & Engineering, Faculty of Civil Engineering & Geosciences, Delft University of Technology, Engineering, Stevinweg 1, 2628 CN Delft, the Netherlands.
E-mail address: m.buisman@tudelft.nl (M. Buisman).

https://doi.org/10.1016/j.jappgeo.2024.105377
Received 10 July 2023; Received in revised form 25 March 2024; Accepted 21 April 2024
Available online 30 April 2024

surveying area and the variation in water temperature, salinity, and (fluid) mud rheology. Because of these variations, even over small distances, re-calibration is often required to acquire a velocity profile for zero-offset measurements, such as echo sounders (Kirichek et al., 2018; Shakeel et al., 2019, 2020).

New surveying techniques are required to tackle the limited temporal resolution and measurement accuracy. Buisman et al. (2022) showed that Distributed Acoustic Sensing (DAS) can be combined with an active source in a laboratory setup to measure the water-mud interface. Rivet et al. (2021)showed that ships can be detected using DAS. We combine both Buisman et al. (2022) and Rivet et al. (2021), and use DAS for nautical depth monitoring in a navigational river channel. We conduct a field study in the Port of Rotterdam and demonstrate how passive noise sources like ships can be used to monitor the nautical depth with optical cables in a horizontal orientation.

1.1. Distributed acoustic sensing

DAS measures the dynamic strain or strain-rate of optical fibers. Optical fibers offer many advantages over conventional electrical sensors, such as electric isolation and immunity to electromagnetic interference, and they are non-conductive and non-corrosive, making them well-suited for utilisation in liquids (Shao et al., 2016; Xu et al., 2017; Yang et al., 2001) and saline environments. Strain or strain-rate can be measured by the changes in photon path length of Rayleigh-backscattered light emitted by a laser source from the same interrogator and measured by a receiver in an interrogator (Lindsey et al., 2020). However, the backscattered signal's phase change has a highly non-linear transfer function causing an ambiguity or an inability to precisely locate the source of the acoustic disturbance, making it unsuitable for seismic applications. Because the phase change is highly non-linear, the phase difference between two points is used instead, referred to as the gauge length (Hartog et al., 2014). Even though the phase difference is averaged over the gauge length, the location of a disturbance along the fiber and waveforms are well preserved. Because of this, DAS measurements have been successfully used in various fields of research, for example, teleseismic earthquake monitoring (Ajo-Franklin et al., 2019; Jousset et al., 2018), vertical seismic profiling (Daley et al., 2016; Martuganova et al., 2021; Mateeva et al., 2014), and earthquake phase identification (Lindsey et al., 2017).

Conventional commercially available instruments use a short-pulse generated by a coherent laser into the fiber (Lindsey et al., 2020). With such a setup, the pulse width limits the spatial resolution. Another drawback of short-pulse systems is the susceptibility to optical non-linearities, such as self-phase modulation and modulation instabilities, which further limits the interrogation-energy output of the laser per pulse and thus limits the backscattered signal (Toulouse, 2005). To monitor large seaports, implying monitoring over large distances with a high spatial resolution, thus poses a problem for short-pulse systems. This is why we selected a system that combines coherent detection with

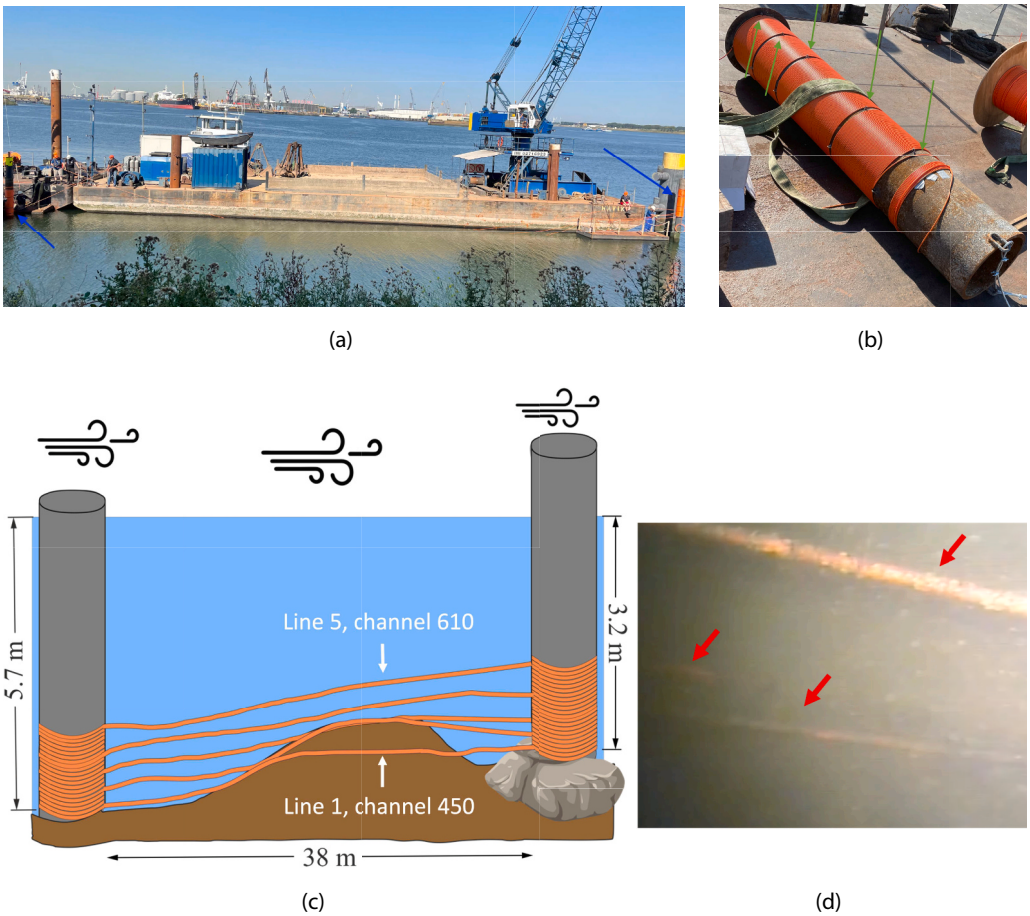

Fig. 1. a): Two mantels with the direct-burial single-mode fiber being lowered onto the steel poles. The blue arrows show the location of the mantles. The platform was used for installation only. b): A photo of a mantel with the fiber. The exposed lines are where rings have been welded on, indicated by the green arrows, that are used to guide the fiber through. These rings are used to create horizontal lines at different heights that can be seen on a). Later the horizontal lines are tightened to reduce cable slacking. c): Sketch of the fiber installation and bathymetry. d): Picture of the dive inspection where line one, the middle line on the left, enters the mud, and lines two and three are on top of the mud. The red arrows show point towards the fibers. (For interpretation of the references to colour in this figure legend, the reader is referred to the web version of this article.)

linear frequency modulation. In such a system, the linear frequency-modulated signal is then compressed using chirp compression techniques, known from radar applications (Richards, 2014), into a short-pulse. By doing so, the interrogator can launch much more energy into the fiber (Wang et al., 2015), allowing it to interrogate much longer distances (Waagaard et al., 2021).

1.2. Field setup

The field setup is situated in the Botlek, located in the Port of Rotterdam, The Netherlands. The setup consists of two 24-m-long steel poles designed to hold a mantel containing the sensing fiber, as shown in Fig. 1. Due to a sharply varying bathymetry, the steel poles were driven in at different depths. One pole was driven at a point with an approximate water depth of 5.7 m, the other - 3.2 m, resulting in lengths exposed to the air of approximately 3 m and 2.4 m, respectively. The distance between the two poles is 38 m.

The mantels are 2.4 m in height and 0.37 m in diameter. Both mantels are coiled with a standard single-mode direct-burial communication fiber with a length of 317 m that covers 1.6 m of a mantle in height, and is connected via a lead fiber of 106 m. As can be seen in Fig. 1 b, rings are welded on the mantel. These rings are used to create horizontal lines. There are five horizontal lines, starting from the very bottom of a mantel at fiber length 423 m (106 m lead fiber +317 coiled on the mantel), then moving up 30 cm twice, then 60 cm, and finally 40 cm, with the final position located on the top of the vertical seismic profile (VSP). The mantels are carefully lowered to prevent the connecting fiber from breaking during installation. A sketch of the setup can be seen in Fig. 1 c.

An ASN OptoDAS interrogator (Waagaard et al., 2021) is used for data acquisition; it converts the fiber into an array of seismic sensors. We use a gauge length, the averaged fiber length for a recording, of 3 m and

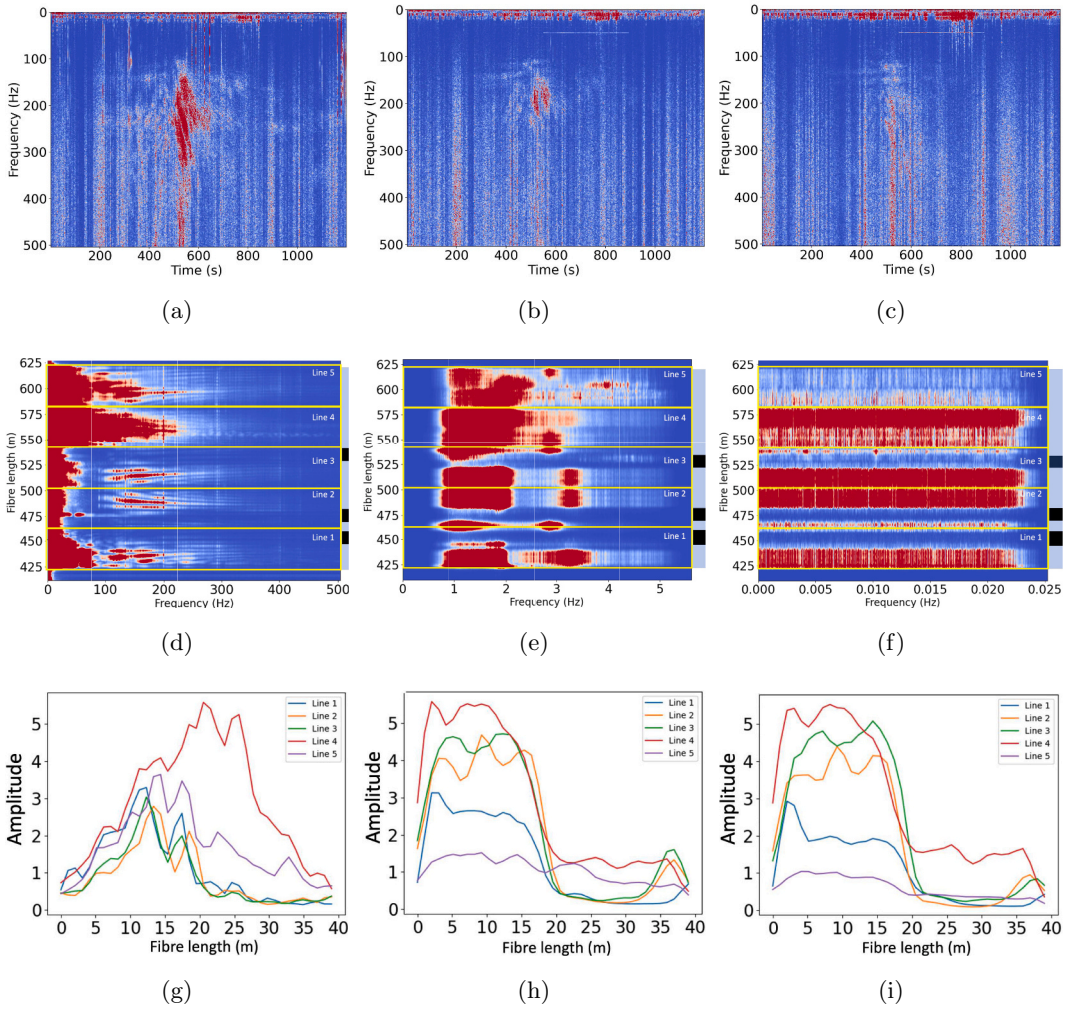

Fig. 2. a): Spectrogram of channel 610, located in water on line 5, with a gauge length of 3 m. The exact location of channel 610 is shown in Fig. 1 c. During this 20-min-long recording, a boat passed between 300 and 800 s. Clear interference patterns can be observed in the shape of hyperbolas that have a mid-point at 500 s. b): Similar to a, but for channel 530, located on line 3, which is pressed against the mud. The same interference patterns as in a can still be observed but are much weaker. c): Similar to Figure a, but of channel 450 located in mud. Similar patterns as in a are observable, but with much smaller amplitudes due to the muting of the signals by mud. Additionally, lower frequencies have larger amplitudes visible than in a and b. d): Power spectral density (PSD) of all five horizontal lines. Each yellow line represents one box, with the first line, denoted by the number"1″ on the bottom right, being the lowest line, which is partly on and in mud, and the fifth line being, denoted by the number"5″ on the top right, being nearest to the water surface. Each line consists of 38 m cable between the poles and 2 m on the poles. Lines four and five exhibit energies with the highest amplitudes. The mud near the right pole can be identified in the PSD as low-amplitude zones, such as at the end of line one, at the beginning of line two, and the end of line three. The water and mud locations are shown on the right of the PSD in blue and black, respectively. e): Like d, but for 0–6 Hz, that likely originates from wind and flow. f): Like d, but for 0–0.025 Hz, which might originate from pole swaying due to wind and currents or seafloor compliance. g:i) Stacked amplitudes of 100 Hz - 504 Hz, 0–6 Hz and 0–0.025 Hz, respectively, along all lines for each meter. The beginning and end of lines two and four have been flipped to make them align with lines one, two and three. (For interpretation of the references to colour in this figure legend, the reader is referred to the web version of this article.)

a channel spacing of 1 m. The 3-m gauge length was chosen because our initial objective was to record surface waves with a short wavelength (Dean et al., 2017).

The OptoDAS interrogator is stored in a shipping container 70 m from the pole setup. We record continuously for 5.7 consecutive days using a 62.5 kHz time sampling, which then is temporally decimated 62 times to reduce data volume.

Finally, a diving inspection is performed to visually validate the locations of the horizontal parts of the fiber.

2. Water-depth estimations based on frequency content

The water-mud interface depth varies in this area because of sedimentation and dredging in the vicinity. Measurement of the depth at a point is thus not representative of the area. Measurement along a line would be much more representative, especially in an area subjected to fluid mud, characterized by its small shear strength. We will show that the wave propagation along a line can be very effectively monitored with high resolution using DAS measurements. One parameter of the propagating waves that can be very useful for monitoring purposes is their amplitude or energy. The energy is influenced by the specific energy loss when propagating through a specific material. We expect a sharp transition in acoustic attenuation due to the muting of cable reverberations by mud (Buisman et al., 2022), as if it were a vibrating guitar string that gets muted by touching the string.

Fig. 2 a shows a power spectral density (PSD) plot of channel 610, located on the fifth line, which is completely suspended in water, on meter 27 from the first pole to the second pole. This figure is calculated using Welch's method (Welch, 1967), and shows that DAS can measure noise from passing vessels with a horizontal fiber. During the recording in Fig. 2 a, one ship passed, which can be observed from 300 to 800 s. Clear constructive and destructive interference patterns in the shape of hyperbolas with high-amplitudes are observable as the ship passes. Interestingly enough, when we compare the same recording of horizontal channels 530 and 450, which are pressed against the mud and buried in the mud, respectively, at the same horizontal distance, we can observe similar patterns, though with significantly lower amplitudes, as shown in Fig. 2 b and c, respectively. This difference in amplitude is further validated when we combine all channels and plot the PSD for the duration of a passing vessel, as shown in Fig. 2 d. In this figure, the start and the end of the five horizontal fibers are indicated by the yellow lines, with the lowest horizontal fiber starting at 423 m and each line consisting of 40 m of fiber, of which 38 m are between the pole, and 2 m are wrapped on the pole. In Fig. 2 d, constructive interference patterns are in the shape of hyperbolas, for example at a fiber length of 500 m. Since the fiber goes from pole one to pole two, then from pole two to pole one, and so on, mirrored frequency patterns can be expected going from an odd to an even-numbered line. This mirroring effect is especially visible at the end of line two and the beginning of line three. The horizontal lines four and five exhibit interference patterns along their complete lengths, whereas lines one, two and three exhibit both high-amplitude constructive interference patterns and low-amplitude zones.

A dive inspection was contracted to inspect the geometry of the lines with special interest for the locations with the low-amplitude zones visually. The recordings made with this dive inspection revealed that line one is buried in mud at the location of these low-amplitude zones, and lines two and three are pressed against consolidated mud at the low-amplitude zones, as shown in Fig. 1 c and in Fig. 1 d. Furthermore, a similar pattern can be observed once we look at lower frequencies likely related to flow and wind waves. Fig. 2 e shows similar high-amplitude zones like Fig. 2 d, but at much lower frequencies (0–6 Hz). In addition, amplitudes around 460 m of fiber length can be observed in this lower-frequency spectrum which is absent for the higher frequencies. The dive inspection revealed that the very end of the mantel is in water because it is installed on top of armour rock, which means that the very end of unevenly numbered lines one and three and the beginning of line two are exposed to water for the first two meters. Intuitively, if the fiber is exposed to water, it will vibrate, and we can measure these reverberations. However, because the cable reverberations for higher frequencies are likely the result of constructive and destructive interference paths in our fiber, and the length from pole two towards the sediments is only two meters, constructive and destructive interference patterns can be formed in this short section.

Finally, when we look over five days at ultra-low frequencies, < 0.03 Hz, we observe very sharp boundaries between high- and low-amplitude zones. Fig. 2 f also exhibits low amplitudes where the fiber is touching or buried in mud, implying that these frequencies are only dominant in water. A reason for this might be due to a temperature difference, making the fiber contract and elongate. This is, however, unlikely because when the fiber is lying on top of the mud, such as for lines two and three, the temperature difference should be (very) similar to that of fiber lines four and five, which are entirely suspended in water, since both are exposed to (almost) the same medium. Furthermore, no temperature change should occur in a period of 50 s.

When we compare lines four and five, we observe high-amplitudes along the complete lines, yet we can separate two zones. The first zone is 20 m near pole one; the second zone is 20 m near pole two. This difference in amplitudes indicates that a possible source for these ultra-low frequencies is either pole swaying caused by wind and currents or seafloor compliance. Because the poles are driven into the subsurface at different locations and depths, they are likely to sway differently with different amplitudes.

3. Data interpretation and application

The muting of various signals by mud gives an exceptional horizontal resolution equal to the fiber's (partial) width. Given that optical cables' widths are often no >1 cm, in our case 6 mm, combined with the strong muting of signals when the fiber is only pressed against mud, the achievable vertical resolution is in the order of mm. In practice, the vertical resolution will be lower since knowing the fiber's exact location is difficult due to, for instance, cable slacking. Nevertheless, the resolution will be high; we expect an order of 5 cm, based the cable slacking with our setup, revealed by gently pulling the horizontal fiber segments during the dive inspection. The horizontal resolution is much lower. The channel spacing of 1 m combined with the gauge length of 3 m limits the obtainable horizontal resolution. We detected the 2 m suspended fiber between the second pole and the, as shown in mud Fig. 1c, giving us a minimum horizontal resolution of 2 m. For monitoring the nautical depth in ports and waterways, the horizontal resolution is, however, far less important than the vertical resolution since sedimentation near quay walls is gradual and lateral changes are seldom smaller than 3 m due to the liquid nature of fluid mud and gradual sedimentation of fine sediments.

Considering that the poles on which the fibers are installed likely act as a resonator is crucial. When we sum the values along the frequencies axes for each of the lines in Figs. 2 d:f, but 0–100 Hz of Fig. 2 d, we obtain Figs. 2 g:i, respectively. In these figures, the resonating effect of the poles is visible by the amplitude drop after 19 m. It shows that the deeper pole (at 0 m horizontal distance) has more prominent resonances than the shallower pole (at 40 m distance). The stacked amplitudes for lines four and five are especially interesting since these lines are entirely suspended in water. Line four shows a clear amplitude drop that can only be related to the pole vibrations since it is completely suspended in water. Line five shows more consistent low amplitudes along the complete line and a smaller amplitude drop, likely due to more cable slacking. Lines one, two, and three exhibit a drop after 20 m to a much lower level than line four. Lines four and five also show a clear drop, but the values of these lines remain higher than the lines touching the mud.

Another way to visualise the difference in frequency content is by subtracting the result in Fig. 2 a from that in Fig. 2 c and visa versa. This way, we obtain the difference panels in Figs. 3 a and b, respectively.

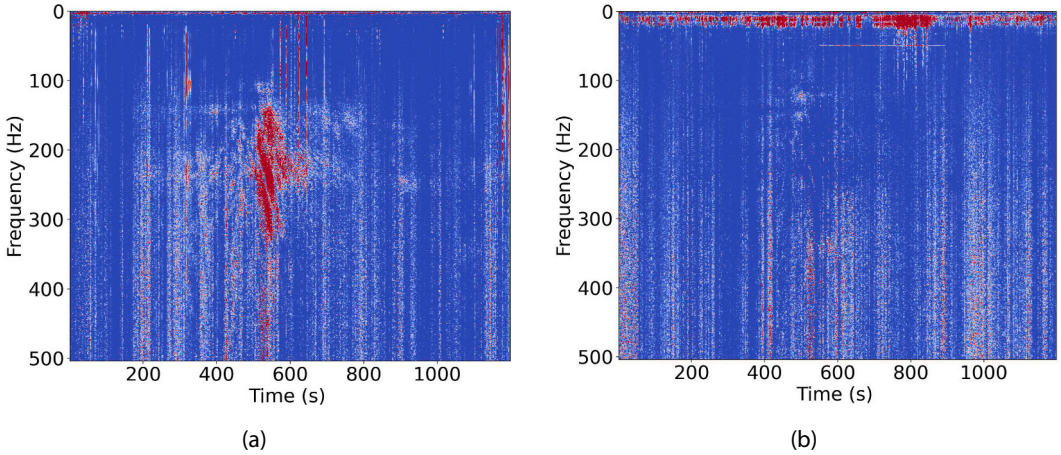

Fig. 3. a): Frequency content of water, calculated by subtracting channel 450, buried in mud and channel 610, located in water, and b) frequency content of mud, calculated by subtracting channel 610 from channel 450.

These figures show that higher signals with frequencies are predominately present in the water, and lower frequencies are predominately present in the mud. A noticeable exception is the frequency of 2.7 Hz, which is related to the resonance of the pole by the wind. This frequency changes with time due to a difference in exposure length of the poles caused by the tidal fluctuations, as shown in Buisman et al., (submitted). This energy propagates down the pole and is muted by mud.

Our DAS measurements along horizontal lines show the potential of monitoring the nautical depth using noise sources. The difference in amplitude zones related to a horizontal fiber being suspended in water, touching or buried in mud, is clearly visible in different frequency ranges. A similar setup could be used in waterways with traffic that generates propeller noise to monitor the nautical depth remotely and continuously. The large difference in amplitudes from noise sources could be used to pick the water-mud interface. The results of this research could be up-scaled for a more elaborate experiment, including a network of horizontal fibers. Based on the recorded signals from passing vessels, water flow, and likely pole swaying or seafloor compliance, a horizontal fiber could be efficiently utilised to monitor the nautical depth using a similar attenuation approach, allowing for a broad coverage without interfering with traffic, as a surveying vessel would.

Fig. 4 shows a possible monitoring DAS setup. In this figure, two lines are installed at different heights, with the lower line buried in mud and the shallower line suspended in water. The interrogator onshore measures small amplitudes for the line in mud and large amplitudes for the line suspended in water. This information is then passed on to the water body authorities via an internet connection. This way, the authorities can map the bathymetry even while a boat is occupying the quay wall and plan to dredge and halt activities for vessels requiring a depth of line C. Alternatively, the port authorities could still allow vessels requiring a depth level of line B without sending a surveying vessel. With this information, quay wall occupation can be improved, (surveying) vessel movements can be reduced, and dredging strategies can be further optimised.

Fig. 4. Potential setup for monitoring the water-mud interface. Here A is an observation station with a DAS interrogator onshore, B is the line suspended in water in this particular situation, and C is a line in (fluid) mud.

A design of this nature could utilize one or multiple passive sources, contingent upon the volume of traffic for signals >50 Hz, the presence or absence of flow for signals within the range of 0.5 Hz to 5.5 Hz, and the proximity to a seashore for signals <0.025 Hz. It is important to note that frequencies might vary at distinct depths or among different structures due to varying interference patterns and resonating frequencies.

In an advanced phase, a Power Spectral Density (PSD) could be developed, integrating machine learning for automated signal processing, converting the frequency spectrum into nautical depth charts.

Additionally, it's important to acknowledge that temporal resolution varies across passive sources. Vessel noise requires the smallest time window, typically a few minutes, whereas pole swaying or seafloor compliance demands the longest, spanning days. This temporal resolution should align with the dynamic environment of the installation. However, for all passive sources, our time window was considerably smaller than the revisiting time of a surveying vessel, typically in the order of two to three weeks (as per internal discussions).

4. Conclusions

Our distributed acoustic sensing (DAS) results showed the potential of using measurements along horizontal fibers for high temporal resolution water-depth monitoring. We showed that this is achieved by using the difference in frequency and amplitude content of signals from noise sources like passing ships and currents in water and mud. The frequency patterns created by passing vessels, > 100 Hz, were clearly visible in a fiber suspended in water and exhibited clear constructive interference patterns. These same patterns were also observed when the fiber was pressed against or buried in mud, yet with much lower amplitudes due to the muting of cable reverberations by mud. In addition, low frequencies, 1 Hz - 5 Hz, showed a similar amplitude spectrum as the higher frequencies from passing vessels. Wind and flow are likely the sources of the lower frequencies, which are notably more pronounced in the fiber suspended in water compared to the fiber placed on or in mud. Furthermore, our findings indicate that the most distinct boundaries between water and mud manifest at ultra-low frequencies, plausibly originating from pole swaying or seafloor compliance. These pronounced transitions can be attributed to the extended recording period of 5.7 days. In contrast, vessel noise, with a recording duration as short as 15 min, exhibits more gradual transitions. This discrepancy in

resolution underscores the inherent trade-off between temporal and spatial resolution.

The advantage of our DAS method over conventional methods is that our method can be used continuously and remotely, given that there is a current, or traffic nearby. The horizontal resolution up to a few mm far outperforms other acoustic/seismic depth monitoring methods. Due to the low cost of optical fibers and the far-reaching dynamic range of interrogators, DAS could be a most attractive alternative for water-depth monitoring using propeller noise or natural currents in shallow marine environments such as ports and waterways. Monitoring the water-mud interface with DAS could resolve temporal resolution problems related to surveying vessel availability and quay wall accessibility at a low expense. With this new monitoring setup, the depth can be monitored without affecting traffic at quay walls. This allows for optimisation of occupancy, increased by reducing surveying vessel movement, and reduced CO2 emissions by optimising dredging strategies.

CRediT authorship contribution statement

Menno Buisman: Writing – review & editing, Writing – original draft, Visualization, Validation, Resources, Project administration, Methodology, Investigation, Funding acquisition, Formal analysis, Data curation, Conceptualization. **Deyan Draganov:** Supervision. **Alex Kirichek:** Supervision.

Declaration of competing interest

The authors declare they have no conflict of interest.

Data availability

The data that support the findings of this study will be made openly available after publication via the TU Delft's repository (https://data.4tu.nl/Delft_University_of_Technology).

Acknowledgment

This project is funded by Port of Rotterdam, Rijkswaterstaat, Hamburg Port Authority and Smart Port and is carried out within the framework of the MUDNET academic network https://www.tudelft.nl/mudnet/.

References

Ajo-Franklin, J.B., Dou, S., Lindsey, N.J., Monga, I., Tracy, C., Robertson, M., Li, X., 2019. Distributed acoustic sensing using dark fiber for near-surface characterization and broadband seismic event detection [Journal Article]. Sci. Rep. 9 (1), 1328. https://doi.org/10.1038/s41598-018-36675-8.

Buisman, M., Martuganova, E., Kiers, T., Draganov, D., Kirichek, A., 2022. Continuous monitoring of the depth of the water-mud interface using distributed acoustic sensing. J. Soils Sediments 22 (11), 2893–2899.

Daley, T., Miller, D., Dodds, K., Cook, P., Freifeld, B., 2016. Field testing of modular borehole monitoring with simultaneous distributed acoustic sensing and geophone vertical seismic profiles at Citronelle, alabama. Geophys. Prospect. 64 (5), 1318–1334. https://doi.org/10.1111/1365-2478.12324.

Dean, T., Cuny, T., Hartog, A.H., 2017. The effect of gauge length on axially incident p-waves measured using fibre optic distributed vibration sensing. Geophys. Prospect. 65 (1), 184–193.

Hartog, A., Frignet, B., Mackie, D., Clark, M., 2014. Vertical seismic optical profiling on wireline logging cable. Geophys. Prospect. 62 (4-Vertical Seismic Profiling and Microseismicity Frontiers), 693–701.

Jousset, P., Reinsch, T., Ryberg, T., Blanck, H., Clarke, A., Aghayev, R., Krawczyk, C.M., 2018. Dynamic strain determination using fibre-optic cables allows imaging of seismological and structural features [Journal Article]. Nat. Commun. 9 (1), 2509. https://doi.org/10.1038/s41467-018-04860-y.

Kirichek, A., Chassagne, C., Winterwerp, H., Vellinga, T., 2018. How navigable are fluid mud layers? [Journal Article]. Terra et Aqua 6–18.

Lindsey, N., Martin, E., Dreger, D., Freifeld, B., Cole, S., James, S., Ajo-Franklin, J., 2017. Fiber-optic network observations of earthquake wavefields: fiber-optic earthquake observations [Journal Article]. Geophys. Res. Lett. 44 (23), 11,792–11,799. https://doi.org/10.1002/2017GL075722.

Lindsey, N., Rademacher, H., Ajo-Franklin, J., 2020. On the broadband instrument response of fiber-optic das arrays [Journal Article]. J. Geophys. Res. Solid Earth 125 (2). https://doi.org/10.1029/2019JB018145 e2019JB018145.

Ma, X., Kirichek, A., Heller, K., Draganov, D., 2022. Estimating p-and s-wave velocities in fluid mud using seismic interferometry. Front. Earth Sci. 10, 251.

Martuganova, E., Stiller, M., Bauer, K., Henninges, J., Krawczyk, C.M., 2021. Cable reverberations during wireline distributed acoustic sensing measurements: their nature and methods for elimination. Geophys. Prospect. 69 (5), 1034–1054. https://doi.org/10.1111/1365-2478.13090.

Mateeva, A., Lopez, J., Potters, H., Mestayer, J., Cox, B., Kiyashchenko, D., Detomo, R., 2014. Distributed acoustic sensing for reservoir monitoring with vertical seismic profiling [Journal Article]. Geophys. Prospect. 62 (4), 679–692. https://doi.org/10.1111/1365-2478.12116.

McAnally, W.H., Friedrichs, C., Hamilton, D., Hayter, E., Shrestha, P., Rodriguez, H., on Management of Fluid Mud, A. T. C, 2007a. Management of fluid mud in estuaries, bays, and lakes. i: present state of understanding on character and behavior. J. Hydraul. Eng. 133 (1), 9–22.

McAnally, W.H., Teeter, A., Schoellhamer, D., Friedrichs, C., Hamilton, D., Hayter, E., others, 2007b. Management of fluid mud in estuaries, bays, and lakes. ii: Measurement, modeling, and management. J. Hydraul. Eng. 133 (1), 23–38.

Richards, M.A., 2014. Fundamentals of Radar Signal Processing. McGraw-Hill Education.

Rivet, D., de Cacqueray, B., Sladen, A., Roques, A., Calbris, G., 2021. Preliminary assessment of ship detection and trajectory evaluation using distributed acoustic sensing on an optical fiber telecom cable. J. Acoust. Soc. Am. 149 (4), 2615–2627.

Shakeel, A., Kirichek, A., Chassagne, C., 2019. Is density enough to predict the rheology of natural sediments? Geo-Mar. Lett. 39, 427–434.

Shakeel, A., Kirichek, A., Chassagne, C., 2020. Rheological analysis of mud from port of Hamburg, Germany. J. Soils Sediments 20, 2553–2562.

Shao, M., Qiao, X., Zhao, X., Zhang, Y., Fu, H., 2016. Liquid level sensor using fiber bragg grating assisted by multimode fiber core [Journal Article]. IEEE Sensors J. 16 (8), 2374–2379. https://doi.org/10.1109/JSEN.2015.2513413.

Toulouse, J., 2005. Optical nonlinearities in fibers: review, recent examples, and systems applications. J. Lightwave Technol. 23 (11), 3625–3641.

Waagaard, O.H., Rønnekleiv, E., Haukanes, A., Stabo-Eeg, F., Thingbø, D., Forbord, S., Brenne, J.K., 2021. Real-time low noise distributed acoustic sensing in 171 km low loss fiber. OSA Continuum 4 (2), 688–701. https://doi.org/10.1364/OSAC.408761.

Wang, S., Fan, X., Liu, Q., He, Z., 2015. Distributed fiber-optic vibration sensing based on phase extraction from time-gated digital ofdr. Opt. Express 23 (26), 33301–33309.

Welch, P., 1967. The use of fast fourier transform for the estimation of power spectra: a method based on time averaging over short, modified periodograms. IEEE Trans. Audio Electroacoust. 15 (2), 70–73.

Xu, W., Wang, J., Zhao, J., Zhang, C., Shi, J., Yang, X., Yao, J., 2017. Reflective liquid level sensor based on parallel connection of cascaded fbg and sncs structure [Journal Article]. IEEE Sensors J. 17 (5), 1347–1352. https://doi.org/10.1109/JSEN.2016.2629488.

Yang, C., Chen, S., Yang, G., 2001. Fiber optical liquid level sensor under cryogenic environment [Journal Article]. Sensors Actuators A Phys. 94, 69–75. https://doi.org/10.1016/S0924-4247(01)00663-X.